Special Folding Pathway to Tetramer Only through the Micelle State of the Corticotropin-Releasing Factor†

Hisayuki Morii,*,‡ Hatsuho Uedaira,‡ Miyuki Ishimura,‡ Shun-ichi Kidokoro,§ Tomokuni Kokubu,‡ and Shinichi Ohashi‡

National Institute of Bioscience and Human-Technology, Tsukuba, Ibaraqi 305, Japan, and Sagami Chemical Research Center, Sagamihara, Kanagawa 229, Japan

Received May 27, 1997⊗

ABSTRACT: The ovine corticotropin-releasing factor (CRF), a peptide hormone of 41 residues stimulating the secretion of adrenocorticotropic hormone, was thermodynamically investigated. By means of size exclusion chromatography and/or ultrafiltration, the CRF solution could be separated into random coil monomers and highly α-helical tetramers, which seem to have amphipathic helix bundle structure. Circular dichroism measurements along with diluting or concentrating the CRF solution revealed that there exists the micelle state above the concentration of 0.1 mM, which would be the critical micelle concentration (cmc). The micelle state was also proved by binding ability for 8-anilino-1-naphthalenesulfonate and endothermic change by dilution across the cmc. The tetramer showed the cooperative thermal transition at about 55 °C in the buffer solution (pH 7.5), so that it would have native-protein-like folding. On the other hand, the micelle undergoes gradual change to dissociated state by heating, regardless of the similar α-helicity to the tetramer. Above the cmc the equilibrium between the tetramer and the micelle takes place as well as that between the monomer and the micelle. Whereas, the direct conversion between the tetramer and the monomer scarcely occurred below the cmc. The titration experiment with 2,2,2-trifluoroethanol (TFE) revealed that the cmc decreases with increasing the concentration of TFE. This tendency is the same as that of general surfactants. Most of experimental results can be well explained by this three-phase model involving the monomer, the tetramer, and the micelle. The lack of the equilibrium between the monomer and the tetramer indicates that the folding pathway of the tetramer is the transformation only through the micelle state and not from the monomer. This pathway resembles the collapse model among the phenomenological models for thermodynamic protein folding. By the mathematical consideration for the dissociation of micelle, we have demonstrated that the expected content of undegradable *k*-mer is $2/(k + 1)$, which agreed well with the observed tetramer content of CRF (40%).

Corticotropin-releasing factor (CRF)[1] is a peptide hormone of 41 residues produced by the hypothalamus. CRF stimulates the secretion of adrenocorticotropic hormone, β-endorphin, and other proopiomelanocortin-derived products from the pituitary. Their physiological roles in mediating stress response have been investigated in detail (Guillemin et al., 1955; Gillies et al., 1979; Sayers et al., 1980; Spiess et al., 1981). Ovine CRF was isolated, and the sequence was identified by Vale et al. (1981).

The amino acid sequence of CRF has potential α-helical amphipathy. However, the secondary structure in aqueous solution is predominantly random coil with very low α-helicity (about 10% or 20%) (Lau et al., 1983; Pallai et al., 1983). On the other hand, ovine CRF was found to form compact secondary structure in the presence of lipid vesicles or at the air−water interface (Lau et al., 1983). These structural features are related to the potential amphipathic region (8−23) (Pallai et al., 1983). The Chou−Fasman prediction of secondary structure (Chou et al., 1978) shows that the region (8−32) (Pallai et al., 1983), or (14−31) (Dathe et al., 1996), is α-helical and the others are not. Circular dichroism spectra in aqueous TFE, which is known as an α-helical structure-inducing solvent, showed that CRF can form highly α-helical conformation. The α-helical regions in aqueous TFE was determined by NMR to be (10−32) (Romier et al., 1993).

One of the most interesting phenomena is the formation of oligomers. It has been reported that two bands bearing ACTH-releasing activity appear in gel filtration experiments of CRF (Schally et al., 1960; Gillies et al., 1979; Sayers et al., 1980; Vale et al., 1981). The larger molecular weight species of CRF elicited higher secretory activity (Vale et al., 1981). The ultracentrifugation experiment indicated that ovine CRF formed the tetramer and that the molecular weight of oligomers gradually increased to that of the octamer depending on concentration (Lau et al., 1983). Dynamic laser scattering study showed that ovine CRF associated with a dimeric Stokes radius at the concentration of 1 mM (Dathe et al., 1996). It seems to be true at a glance that CRF undergoes the concentration-dependent association. How-

† This work was supported by grants-in-aid from the Agency of Industrial Science and Technology, MITI.

* To whom correspondence should be addressed. Tel.: +81-298-54-6184. Fax: +81-298-54-6194.

‡ National Institute of Bioscience and Human-Technology.

§ Sagami Chemical Research Center.

⊗ Abstract published in *Advance ACS Abstracts,* November 15, 1997.

[1] Abbreviations: CD, circular dichroism; CRF, corticotropin-releasing factor; Fmoc, 9-fluorenylmethoxycarbonyl; TFA, trifluoroacetic acid; HPLC, high-performance liquid chromatography; ESI-MS, electrospray ionization mass spectroscopy; SEC, size exclusion chromatography; Da, dalton; ITC, isothermal titration calorimetry; DSC, differential scanning calorimetry; TFE, 2,2,2-trifluoroethanol; ANS, 8-anilino-1-naphthalenesulfonic acid; cmc, critical micelle concentration.

S0006-2960(97)01229-4 CCC: $14.00

ever, the change of CD spectra dependent on the peptide concentration has not yet been elucidated on the basis of association equilibrium between monomer and oligomer. In contrast with CRF, several amphipathic designed peptides were shown to undergo monomer−oligomer association depending on the concentration (Ho et al., 1987; Betz et al., 1996). The quite different behavior of CRF from these peptides is strange and interesting.

Thus in this work we focused on the mysterious oligomer formation of ovine CRF. Using size-exclusion chromatography (SEC), CD, fluorescence, isothermal titration calorimetry (ITC), and differential scanning calorimetry (DSC), the isolated monomeric and oligomeric species of ovine CRF were investigated in detail. Thermodynamic studies enabled us to prove that three states of ovine CRF, i.e., monomer, oligomer, and micelle, can be recognized. As described later, the oligomeric CRF was composed of the tetramer alone. From the viewpoint of protein folding, CRF provides the interesting case that the folding course is not simply dependent on the concentration.

EXPERIMENTAL PROCEDURES

Materials

Ovine CRF with an amide-type C-terminus was synthesized by a usual solid phase method using Fmoc-strategy with ABI-430A peptide synthesizer (Applied Biosystems, USA). The peptide was cleaved from the resin using trifluoroacetic acid (TFA) containing 1,2-ethanedithiol and water as cation scavengers and then purified by reversed-phase HPLC using water−acetonitrile eluent system containing TFA (Ohashi et al., 1983). Purified CRF was lyophilized twice from aqueous solution to remove excess TFA. By the analysis of ESI-MS with API-III (Perkin-Elmer Sciex Instruments, USA) the molecular weight was shown to be 4670.0, which proved the correct product (theoretical molecular weight: 4670.4). The peptide concentration was determined with the result of quantitative amino acid analysis, from which the extinction coefficient was estimated to be 1050 M^{-1} cm^{-1} at 220 nm and used for further studies.

CRF was dissolved in 10 mM sodium phosphate buffer (pH 7.5) just before use, because the peptide is easily to be concentrated at the air−water interface (Lau et al., 1983) or the surface of vessels on prolonged keeping in a solution.

Size Exclusion Chromatography and Ultrafiltration

Size exclusion chromatography was performed on a Superdex 200 (prep. grade, Pharmacia) column (1.5 × 70 cm), a Sephadex G50 (fine grade, Pharmacia) column (1.5 × 110 cm), and TSKgel G3000PW HPLC column (Toso, Japan) (0.75×60 cm). CRF was dissolved in sodium phosphate buffer (pH 7.5) and loaded onto each column, which was eluted with the same buffer solution at room temperature. The eluted peptide was monitored by the absorption at 220 nm. Lactate dehydrogenase, albumin, ovalbumin, chymotrypsinogen A, trypsin inhibitor, and ribonuclease were used as the molecular weight standards, which were purchased from Pharmacia.

To separate the monomer and oligomer of CRF conveniently, a Centricon 30 ultrafiltration filter (Amicon, USA) with a molecular cutoff mass of 30 kDa was used. For this purpose, the concentration of loaded solution was about 0.01 mM and 95% of the solution volume was filtrated, while to concentrate the CRF solution, a Centri/Por (cutoff, 3.5 kDa) (Spectrum Medical Ind., USA) filter was used.

Circular Dichroism Measurement

CD spectra were measured with Jasco J-600 spectropolarimeter in quartz cuvettes equipped with water jacket to control the temperature. The cuvettes with the path lengths of 0.2, 0.5, 1, 2, 5, and 10 mm were used, depending on the peptide concentrations. Thermal transition was measured by simultaneously monitoring the temperature of circulating water and the molar ellipticity at 222 nm, which is the typical band of α-helix. The temperature, thus measured, was confirmed to be identical to that of sample solution within the error of 0.5 K by the other experiments. The titration by the addition of 2,2,2-trifluoroethanol (TFE) was manually carried out with pipettes at 20 °C.

Calorimetry

Differential scanning calorimetry (DSC) measurements were performed with MicroCal MCS microcalorimeter. The same sodium phosphate buffer solution was used in its reference cell. The heating rate was 1.0 K min^{-1}. The observed heat capacity curves were analyzed by the method developed by Kidokoro et al. (1987, 1988).

Isothermal titration calorimetry (ITC) was carried out for measuring dilution heat effect with ITC unit of the same microcalorimetry system. The small portions of CRF solution in the buffer were added stepwise into the cell filled with the same buffer at 25 °C. The peaks of the obtained thermograms were integrated with the ORIGIN software.

Fluorescence

The fluorescence of 8-anilino-1-naphthalenesulfonic acid (ANS) was measured in the presence of various concentrations of CRF with a Shimadzu RF-5000 spectrofluorometer. The concentration of ANS was 10 μM, and a cuvette with 1 mm path length was used to detect even weak affinity. Using the excitation wavelength at 350 nm, the fluorescence spectra were recorded at 20 °C with the emission band width of 5 nm.

RESULTS AND DISCUSSION

Size Separation of CRF

The size exclusion chromatography (SEC) of the chemically synthesized CRF gave two major peaks as shown in Figure 1. This result is similar to that for CRF extracted from natural source (Vale et al., 1981). This means that the oligomerization occurs even in non-natural systems. The first peak eluting faster was found to be the molecular weight of 11-mer of CRF, using linear calibration with the molecular weight standards (Figure 1). However, by means of sedimentation equilibrium, it was already reported that the oligomeric species would be a tetramer and its larger associates (Lau et al., 1983). The difference in the oligomeric numbers by sedimentation and our SEC measurements can be explained as that the molecular form of oligomeric CRF is not a sphere but rod-like shape. This behavior is known for longitudinal molecules such as coiled-coil peptides (Lau et al., 1984). The second peak shows the molecular weight of monomeric CRF. The widths of both peaks were

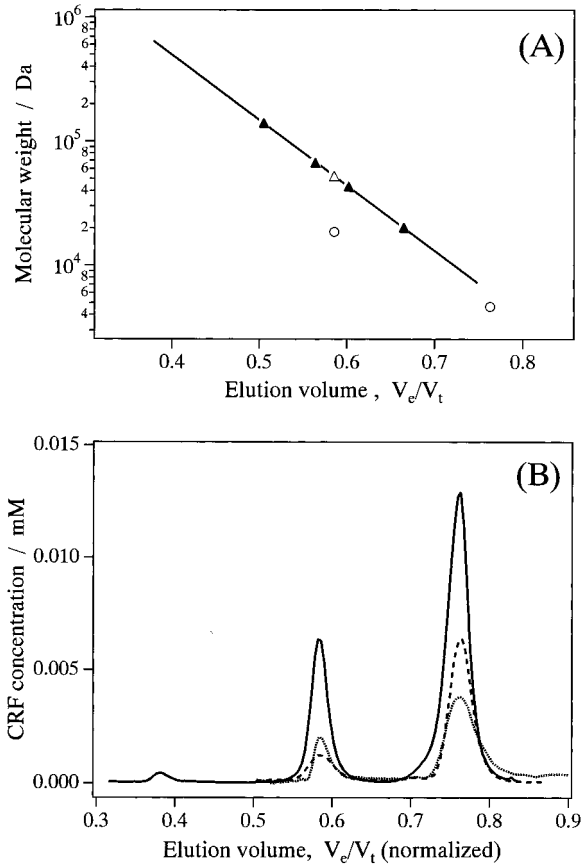

FIGURE 1: (A) Calibration curve for molecular weight in the size exclusion chromatography with Superdex 200 column. The calibration curve was obtained by the least-squares method for the elution volumes of the standard proteins, which are lactate dehydrogenase (molecular weight, 139 900), albumin (67 000), ovalbumin (43 000), and trypsin inhibitor (20 100). The data were plotted for these standard proteins (closed triangles), CRF composed of the monomer and the tetramer (open circles), and the imaginary 11.3-mer of CRF (open triangle). V_e and V_t represent the elution volume of samples and the column volume, respectively. (B) Comparison of the elution profiles of size exclusion chromatography at room temperature. The chromatograms were recorded by detecting the absorbance at 220 nm and converted to CRF concentration as shown. The chromatography was performed on Superdex 200 (solid), TSKgel G3000PW (dashed), and Sephadex G50 (dotted) columns, to which the CRF solutions were loaded at the concentrations of 0.74, 0.03, and 0.05 mM, respectively. The scale of abscissa was that for Superdex 200. The elution profiles were normalized horizontally to have the same elution volumes of the monomer and the tetramer despite the difference in the columns applied.

equally narrow and were as sharp as those of the proteins used as standard. Therefore, the oligomeric CRF is a unique species and is not a mixture of oligomers with different association numbers. Thus, we assume that the oligomeric CRF is a tetramer according to the result of sedimentation equilibrium as above.

The contents of tetrameric CRF estimated from the peak areas for several runs gave various values in the range of 20−35%. There seemed to be little correlation between the tetramer contents and the initial CRF concentrations in the loaded solutions when the CRF concentrations were below 0.1 mM in the eluted solution. Even in the experiments with the other columns described in Experimental Procedures, the similar tetramer contents (20−35%) were obtained. Thus the abundance of tetrameric species seems to be irrespective of SEC conditions. Since the standing experiments revealed that the highly diluted CRF solution is quite susceptible to

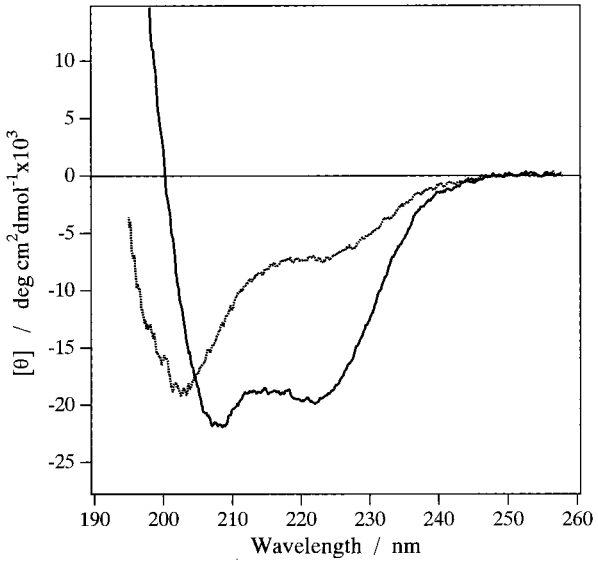

FIGURE 2: Circular dichroism spectra of the monomer (dotted line) and the tetramer (solid line) of CRF. CD spectra of 0.007 mM monomer and 0.0013 mM (monomer unit) tetramer, which were isolated by means of size exclusion chromatography with Superdex 200, were measured at 20 °C in cuvettes with path lengths of 5 and 10 mm, respectively. The buffer solution of 10 mM sodium phosphate (pH 7.5) was used for a series of experiments.

possible interface denaturation, the variety of the tetramer content (20−35%) may be attributed to this instability of the CRF solution. A tetramer content higher than the range above was never observed. The essential tetramer content of the simply dissolved CRF solution may be determined *a priori*.

The peaks of monomeric and tetrameric CRF are well apart, and no intermediate elution band was observed. Also, the fractionated solution containing either monomer or tetramer caused no conversion between the monomer and the tetramer. This means that the equilibrium between the monomer and the tetramer is extremely slow or actually negligible in the course of passing through the column.

The small peak at 0.39 of SEC with Superdex 200 corresponds to the exclusion limit of the column (Figure 1). Since the concentration of the eluted solution is fairly lower than 0.1 mM, which is the critical micelle concentration (cmc) as discussed below, this peak would be due to nonequilibrium micelles including some contamination.

Because the apparent molecular mass of CRF tetramer is 50 kDa as shown in Figure 1, an ultrafiltration membrane with the cutoff molecular mass of 30 kDa was conveniently employed to separate the monomer and the tetramer. The filtrate and the remained solution after ultrafiltration gave the CD spectra consistent with those of monomeric and tetrameric CRF solutions fractionated by SEC, respectively. This result shows the availability of ultrafiltration membrane for the separation of these species. Also, it was again proved that the tetramerization of CRF was not a usual equilibrium phenomenon between monomer and tetramer.

CD Spectra of CRF in Buffer Solution

The CD spectrum of CRF monomer exhibited a relatively large negative band at 208 nm and a small negative band at 222 nm (−7000 deg cm^2 dmol^{-1}) (Figure 2). The helicity of monomeric CRF seems to be about 20% on the basis of the intensity at 222 nm, roughly estimated by the method of

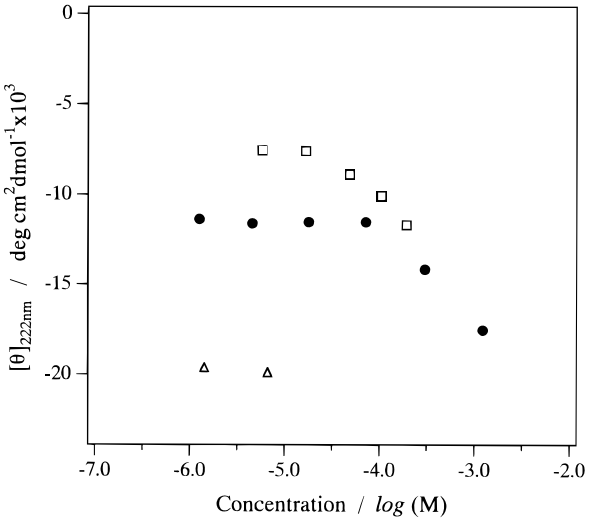

FIGURE 3: Concentration dependence of the molar ellipticities at 222 nm of CRF solutions at 20 °C. The molar ellipticities of simply dissolved CRF solutions (closed circles) were measured along the dilution. Those of the isolated monomer (open squares) and tetramer (open triangles) were measured along concentration by ultrafiltration. CD spectra were measured in the quartz cuvettes with appropriate path lengths from 0.2 to 20 mm.

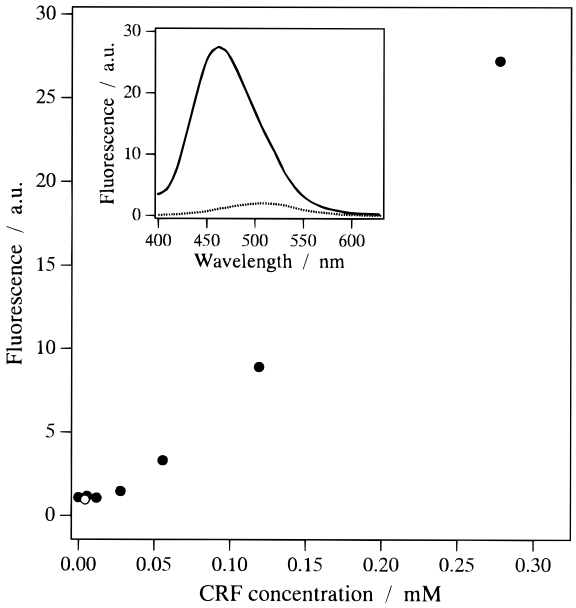

FIGURE 4: Fluorescence of ANS in the presence of various concentrations of CRF. The fluorescent intensities at 464 nm of the simply dissolved CRF solutions (closed circles) and the isolated tetramer solution (open circle) containing 0.01 mM ANS in each were plotted against CRF concentrations. The inlet represents the fluorescence spectra of 0.28 mM CRF solution and the control. The sample solutions were incubated for about 20 min after mixing the CRF solutions and 0.1 mM ANS stock solution. Fluorescence measurements were carried out at 20 °C with the excitation wavelength at 350 nm.

Chen et al. (1974). The monomer would be mainly random coil structure.

On the other hand, the tetramer gave the CD spectrum of typical α-helix-rich structure (Figure 2). The molar ellipticity at 222 nm was −20 000 deg cm^2 dmol^{-1}. Assuming that the peptide has no β-structure, the α-helix content was estimated to be 60%. This high α-helicity can be attributed to potential amphipathy of the sequence as suggested previously (Pallai et al., 1983). The amphipathic helix would cause oligomerization, which is probably a helix-bundle formation. The α-helix content of 60% corresponds to 25 residues of the helical chain length. While, this is somewhat larger than potential amphipathic sequence, which is presumed to be the region (7−22) by the estimation method for amphipathic helical propensity (Morii et al., 1997). The additional α-helix may be formed at the neighboring region (23−32), which is proposed to be α-helical by Chou−Fasman method (Pallai et al., 1983).

The CD spectrum of c.a. 0.01mM CRF solution prepared by dissolving the peptide powder showed the intermediate pattern of those for the monomer and the tetramer. The spectrum could be well fitted with the linear combination of these. Taking into account the results of SEC experiments as well, it is obvious that the simply dissolved CRF solution contains both monomeric and tetrameric species of CRF.

Concentration Dependence of CD Spectra

The lyophilized peptide was dissolved in the buffer solution and the CD spectra were measured at the several diluted concentrations. As shown in Figure 3 the molar ellipticity at 222 nm decreased with dilutions down to 0.1 mM, while, at concentrations below 0.1 mM it became nearly constant about −12 000 deg cm^2 dmol^{-1}. The monomeric and tetrameric CRF solutions prepared by ultrafiltration gave both constant molar ellipticities below 0.02 mM. The tetramer did not change to the monomer even by further dilution. This means that the equilibrium does not exist among the monomer and the tetramer at the low concentration as mentioned above. On the other hand, when the solution of CRF monomer was concentrated to over 0.05 mM, the molar ellipticity increased and coincided with the line of simply dissolved CRF solution. This concentration dependent change is likely to be due to the appearance of some associated species. The concentrated solution of the monomer once above 0.1 mM underwent the similar change in diluting as the simply dissolved solution.

In detail, the turning point of the simply dissolved solution is not consistent with that of the separated monomer solution. This may be attributed to the heterogeneity in the separation tube because the ultrafiltration causes somewhat high concentration locally near the membrane. Even at an average concentration below 0.1 mM, the monomer solution after concentration would contain the portion once raised over 0.1 mM, which resulted in the solution containing both monomer and tetramer. Thus, the molar ellipticity of the monomer solution increased with concentration even at the concentration below 0.1 mM.

ANS Binding Experiment

The fluorescence intensity of ANS at 464 nm was plotted at various concentrations of CRF as shown in Figure 4. At a concentration below 0.03 mM the fluorescent enhancement was not observed. However, above 0.1 mM the steep increase in fluorescence occurred with the blue shift of maximum emission wavelength. The intensity change is not linear for the CRF concentration, and the turning point calculated by extrapolation (about 0.05 mM) is a little smaller than the result of CD. ANS molecules may induce the micelle formation even below 0.1 mM. The strong fluorescence at the higher concentration than 0.05 mM is due to the incorporation of ANS into hydrophobic environment,

which would be provided by the micelle formation. The wavelength of maximum emission was 464 nm at 0.28 mM. Therefore, the micelle has molten globular characteristics, because molten globule proteins give emission maxima between 470 and 492 nm (Handel et al., 1993). The slope at the region below 0.03 mM is almost level, so that the affinity of the tetramer for ANS is negligibly low. The result of the isolated tetramer solution is in line with this. Thus, the tetramer exhibits quite different feature from the micelle in spite of their similar α-helicity. The tetramer seems to be rigid enough to prevent ANS from binding. This means that the folding type of the tetramer is not molten globular but native-protein-like.

ITC Measurement of Dilution

The direct measurement of enthalpy change in dilution by ITC also enabled us to distinguish the micelle state from the tetramer. Dilution from 1.3 to 0.01−0.04 mM was an endothermic course ($\Delta H \cong 10$ kJ mol^{-1}). On the other hand, dilution from 0.04 to 0.0005−0.002 mM showed exothermic changes ($\Delta H \cong -40$ to -25 kJ mol^{-1}), of which the enthalpy changed depending on the dilution ratios. The former, i.e., the dilution across 0.1 mM, can be attributed to the hydration of hydrophobic moiety, which would be most probably caused by the dissociation of CRF micelles. The latter is analogous to the simple dilution of general solutes, which involves no dissociation change.

Temperature-Scanning CD Measurement of CRF

The thermal denaturation behaviors were measured for various concentrations of CRF by means of temperature-scanning CD and DSC. The CRF solutions were prepared by simply dissolving as above. At the concentration of 0.005 mM, the sharp transition in molar ellipticity at 222 nm ($[\theta]_{222}$) was observed (Figure 5A). In the folded state below 40 °C, the molar ellipticity decreased slowly in magnitude with increasing the temperature, while in the denatured state above 65 °C, it had little change and became constant at −6000 deg cm^2 dmol^{-1}. This transition behavior resembles that of α-helical coiled-coil peptides (Morii et al., 1997). On the other hand, the transition curve at 0.3 mM was much different from that at 0.005 mM. The apparent transition temperature changed up to 65 °C at 0.3 mM. Additionally, the values of $[\theta]_{222}$ decreased in magnitude in both folded and denatured states. These two types of transition curves bordered at about 0.1 mM, which can be well recognized in the plots of the concentration dependence of transition temperature (Figure 5B). The border concentration is in accord with that for molar ellipticity as described in the previous section.

The transition at the concentration below 0.1 mM is due to that of the tetramer alone, because the monomer hardly undergoes the thermal transition (data not shown). This is also supported by the facts that the transition temperatures are constant irrespective of the CRF concentrations and that the transition curve of the isolated tetramer solution closely resembled that of the solution below 0.1 mM except for the intensity. This constancy of transition temperature means that the transition is not reversible, because the reversible transition between tetramer and monomer generally shows concentration-dependent transition temperature.

While, at the higher concentration than 0.1 mM, the gradual decrease in $[\theta]_{222}$ intensity with increasing the temperature was observed. This non-cooperative change would be attributed to the partial dissociation of CRF micelles. Another possibility, i.e., that there occurs intramicelle conversion such as α-helix to random structure, is less probable because the intramicelle change could easily cause some cooperative transition. The gradual decrease in molar ellipticity occurred even above the temperature of the partial sharp transition, e.g., 73 °C for 1.2 mM CRF solution. Thus, the micelle species generated above 0.1 mM gave a characteristic change along the wide temperature range, so it is explicitly distinguished from the tetramer.

Also at the concentration above 0.1 mM, the partial sharp transition occurred at higher temperature than that below 0.1 mM, which can be attributed to the unfolding of the tetramer co-existing with micelles. Apparent transition temperatures increased as the CRF concentration increased. The tetramer may be stabilized by the aid of the micelles because the micelles are generally formed by the amphiphilic interactions and often interact with amphiphiles. The equilibrium between the tetramer and the micelles would contribute this. These results revealed that there exist two equilibria. One is the equilibrium between the monomer and the micelle, and another is between the tetramer and the micelle.

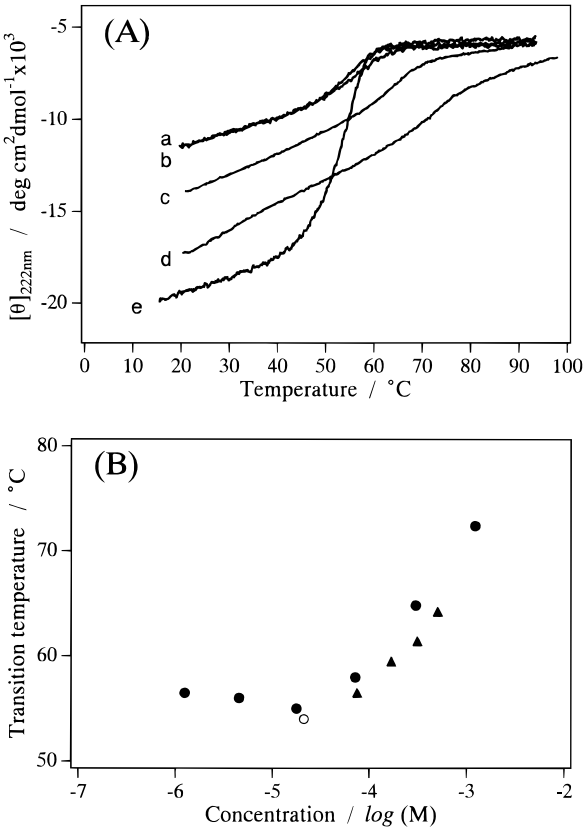

FIGURE 5: (A) Temperature dependence of the molar ellipticities for various CRF solutions at 222 nm. The molar ellipticity at 222 nm was monitored with increasing the temperature at the rate of 1.0 K min^{-1}. The CRF concentrations were 0.005 (a), 0.07 (b), 0.30 (c), and 1.2 mM (d). The data for the isolated CRF tetramer (e) at 0.02 mM were superimposed. (B) Dependence of apparent transition temperatures on the CRF concentrations. The transition temperatures obtained by temperature-scanning CD and DSC were shown with closed circles and closed triangles, respectively. The transition temperature was defined as the position with half-native fraction for sharp transition in temperature-scanning CD. For DSC the peak temperature was adopted as the transition temperature because of difficulty in analysis. The transition temperature of isolated tetramer (open circle) determined by CD was also plotted.

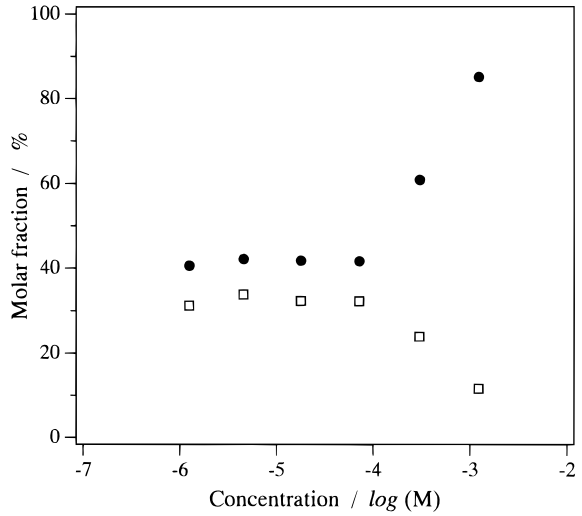

FIGURE 6: Concentration dependence of the molar fraction of the non-monomeric species (closed circles) at 20 °C and the tetramer (open squares) at the transition temperature. All the plots are for simply dissolved CRF solutions. The molar fraction of non-monomeric species, i.e., the tetramer and the micelle, was calculated on the basis of the molar ellipticity at 222 nm at 20 °C on the assumption that the molar ellipticity of the micelle is the same as the tetramer. The molar fraction of the tetramer was determined at each transition temperature using the relative amount of the step height corresponding to the sharp transition in CD measurement. At concentrations below 0.1 mM, the difference in the molar fractions obtained by both methods is mainly attributed to the temperature difference.

Since the apparent sharp transition is caused by the tetramer, it is reasonable to estimate that the step height in molar ellipticity of this thermal transition corresponds to the molar fraction of the tetramer (see Figure 6). When the slopes at both sides of the transition are extrapolated, the step height can be evaluated. At 20 °C, the differences between these two extrapolated lines for the data at various concentrations roughly agreed with one another. It is likely that the potential content of the tetramer is almost consistent irrespective of the concentration. This tetramer content decreased as the temperature was increased and seems to disappear at over 100 °C.

Assuming that the molar ellipticity at 222 nm of CRF micelle is the same as that of the tetramer (−20 000 deg cm^2 dmol^{-1} at 20 °C), it is possible to evaluate the sum of molar fractions for the tetramer and the micelle. This assumption would be valid to some extent because the molar ellipticity at 222 nm in 50% aqueous TFE is −25 000 deg cm^2 dmol^{-1} and seems potentially maximal. Using the extrapolation of the slope for the folded state of the isolated tetramer, the molar ratios of the tetramer and the monomer were calculated (Figure 6). Below the concentration of 0.1 mM the CRF solution consists of its monomer and tetramer. The negligible equilibrium between monomer and tetramer results in their constant molar fractions regardless of the concentrations. Above 0.1 mM, the molar fraction of the micelle state increased remarkably; nevertheless, the molar ratio of monomer and tetramer does not change so much even in the presence of the micelles.

Below the concentration of 0.1 mM, the molar ellipticity was not recovered at all even when the heat-treated CRF solution was cooled to room temperature. Similarly to above discussions, the monomer cannot form the tetramer in the absence of the micelles. On the other hand, above 0.1 mM

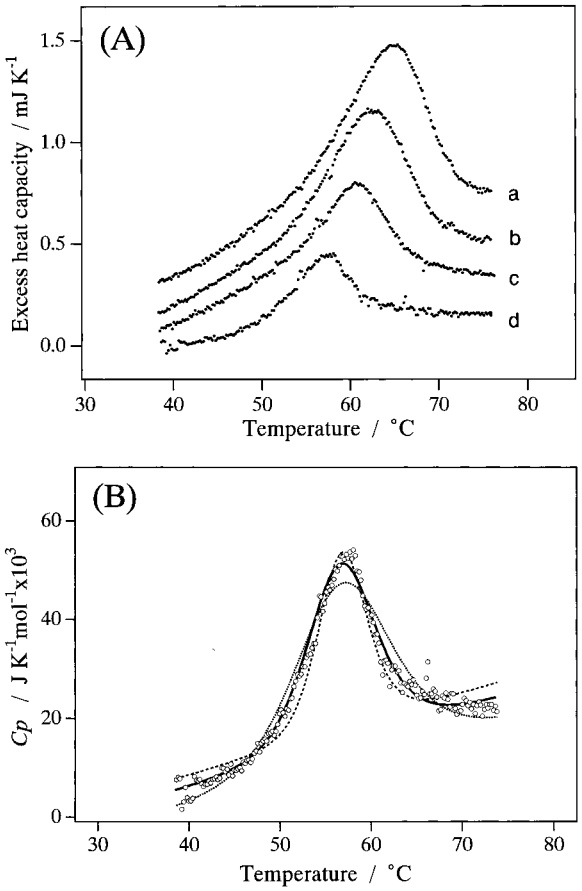

FIGURE 7: (A) Excess heat capacity of CRF solutions. The DSC was measured for the CRF solutions at the concentrations of 0.51 (a), 0.31 (b), 0.17 (c), and 0.08 mM (d), using a heating rate of 1.0 K min^{-1}. Because the CRF monomer gave no transition in CD measurement, the excess heat capacity was expressed in mJ K^{-1} without taking into account the concentration. (B) The observed and the calculated DSC curves for 0.08 mM CRF solution. Assuming that the content of the tetramer is 40% below the concentration of 0.1 mM, the observed DSC data (open circles) were corrected so as to be the heat capacity per net tetramer. The curves for dimer (dotted), tetramer (solid), and octamer (semi-dashed) models, which relate to 0.016 mM dimer, 0.008 mM tetramer, and 0.004 mM octamer, respectively, were calculated according to the equations of two-state transition. The difference in heat capacity between the folded and the unfolded states was set to be zero, because it was difficult to estimate due to probable interference of the micelles. The actual vertical scale for the dimer model is one-half of the apparent scale, and that for the octamer model is twice that of the apparent scale. The calculated calorimetric enthalpy was 258, 362, and 509 kJ mol^{-1} for the dimer, tetramer, and octamer models, respectively.

the thermal transition is highly reversible. This was shown by not only CD but also DSC. The tetramer would be formed only through the dissociation of the micelles.

DSC Analysis

DSC measurements of simply dissolved CRF solutions were performed in the concentration range from 0.08 to 0.51 mM (Figure 7A). The temperatures of transition peaks increased with increasing the CRF concentration. The feature of the thermal transition was compatible with the results of temperature-scanning CD measurements. The CRF concentrations used for DSC are near or above 0.1 mM, so that the solutions would contain the micelles at least in the cases above 0.1 mM. When the observed DSC curves were corrected with the total concentration of CRF, each major

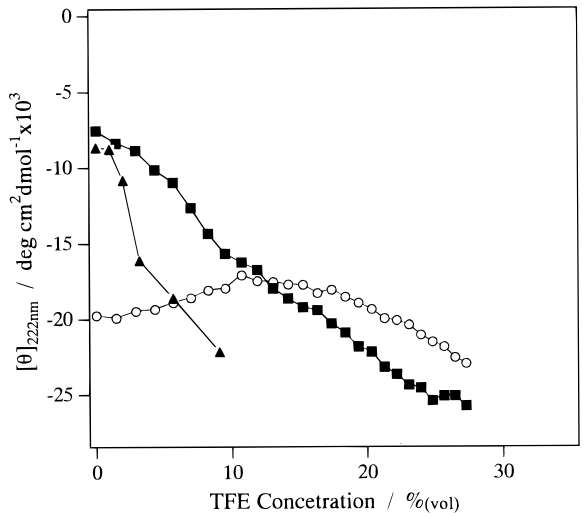

FIGURE 8: TFE titration curves of CRF solutions determined by molar ellipticity at 222 nm. TFE was added stepwise to the isolated 0.007 mM tetramer (open circles), 0.006 mM monomer (closed squares), and 0.057 mM monomer (closed triangles) solutions. TFE concentration was defined as the volume % of TFE to the sum of the buffer and TFE volumes. The CRF concentration at each TFE content was corrected by the total volume of the mixed solvent.

transition showed an apparent transition enthalpy of ~20−40 kJ (monomer mol)$^{-1}$, which was roughly estimated. This enthalpy value is fairly small in comparison with the van't Hoff enthalpy calculated for the data of temperature-scanning CD measurements, which ranged from 310 to 390 kJ mol^{-1} at several CRF concentrations. This result can be explained by the intermolecular cooperativity in the transition as well as by the low content of the tetramer.

Because the main transition corresponds to the unfolding of the tetramer, the excess heat capacity curve at 0.08 mM was analyzed by the use of thermodynamic equations (Kidokoro et al., 1987, 1988). Assuming the tetramer content to be 40%, the theoretical curves of two-state transition with 2-to-2, 4-to-4, and 8-to-8 stoichiometry were calculated and superimposed on Figure 7B. The 4-to-4 model, which represents the transition from a folded tetramer to a random-coil tetramer, well elucidates the observed transition curve. The transition enthalpy was evaluated to be 360 kJ (net tetramer mol)$^{-1}$ on the assumption that the tetramer content is 40%. This enthalpy agreed with that by temperature-scanning CD, and the 4-to-1 model also fit. It was unclear whether the denatured state was the tetramer or the monomer. However, we can certainly conclude that the oligomeric species is the tetramer and that the main transition is due to its unfolding. The apparent van't Hoff enthalpies are consistent in spite of the CRF concentrations as mentioned above, so that the broadening of the endothermic peak at the higher CRF concentrations suggests that there exists non-cooperative intermolecular interaction, which would be the equilibrium between the tetramer and the micelle.

Structural Changes by the Addition of Trifluoroethanol

The α-helicity of the isolated monomer solution increased by the addition of TFE (Figure 8). Interestingly, the steep increases in α-helicity of 0.006 and 0.057 mM CRF monomer solutions occurred at the different TFE concentrations. Such concentration dependence can usually be attributed to the association of the monomer, while TFE is known as a solvent inducing α-helix, which is generally well solvated and independent without forming bundle structures. The CD spectrum of CRF monomer at 30% TFE exhibited a larger band ratio at 208−222 nm, comparing with the CD of tetramer solution without TFE. Therefore, in 30% TFE solution CRF seems to exist as independent α-helices. Summarizing the results, it is concluded that the isolated monomer of CRF undergoes three-state change in the TFE concentration range from null to 30%. For example, 0.006 mM CRF monomers form the micelle at about 8% TFE, where the micelle system would contain the monomer and the tetramer as well, and they change to independent α-helical monomers at about 25% TFE.

The TFE concentration, at which the micelles emerge, is 2.5% for 0.057 mM CRF monomer. In other words, the critical micelle concentrations are 0.1, 0.05, and 0.005 mM of the monomer in 0%, 2.5%, and 8% TFE solutions, respectively. This tendency that the addition of alcohol lowers the critical micelle concentration is the same phenomenon as generally observed in surfactants (Herzfeld et al., 1950).

Statistical Model for Dissociation to the Tetramer

In order to elucidate the specific formation of the tetramer at the stage of dilution, we have assumed the statistical model as follows: (i) the micelle consisting of the monomers dissociates stepwise at random positions; (ii) each monomer can be conveniently numbered as in the one-dimensional array; and (iii) the dissociation proceeds until giving monomeric species except for forming tetramer, which causes no more dissociation. Here, we introduce the function $P_{n,k}$, which represents the statistically expected molar fraction of undegradable k-mer generated by the dissociation of n-mer micelle. In this expression the unit of mole is defined as the amount of the monomer. In considering the concrete case, for example, of $n = 6$ and $k = 4$, the first dissociation results in the paired fragments, 1+5, 2+4, 3+3, 4+2, and 5+1, with the same probability. Among these two, 4-mers are obtained as the molar fraction of 4·2/(6·5). The remaining two 5-mers are susceptible to further dissociation potential to form 4-mers, so that the expected molar fraction of this course can be calculated by multiplying $P_{5,4}$ by the molar fraction of tetramer, 5·2/(6·5). Therefore, we obtain the equation, $P_{6,4} = 4\cdot2/(6\cdot5) + P_{5,4}\cdot5\cdot2/(6\cdot5)$. In a similar manner, the general equation can be expressed as the following:

$$P_{n,k} = \frac{2k}{n(n-1)} + \sum_{f=k+1}^{n-1} (mP_{m,k}) \frac{2}{n(n-1)}$$

This equation can be simplified to the form, $P_{n,k} = P_{n-1,k}$. Since the value $P_{k+1,k}$ is calculated to be $2k/\{k(k+1)\}$ similarly as described above, the final equation is represented as $P_{n,k} = 2/(k+1)$.

For the case of CRF, which was proved to form the tetramer, the molar fraction of the tetramer is expected to be $2/(4+1) = 0.4$ using the above equation. The expected value is fairly in harmony with the experimental values as shown in Figure 6. This statistical model may be somewhat idealized, however, and it may be concluded that the tetramer formation is based on the random dissociation mechanism.

CONCLUSION

The spectrometric and thermodynamic measurements revealed that CRF forms the micelle above 0.1 mM which

co-exists with the monomer and the tetramer. In the micelle state CRF has highly α-helical structure. By dilution of the CRF micelles, both the monomer and the tetramer emerged at once with a constant molar ratio. The tetramer content below the concentration of 0.1 mM was not changed even by the further dilution. This means that the tetramer is not in an equilibrium relationship with the monomer in contrast with the micelle system. The irreversibility in the thermal process below 0.1 mM also supports this phenomenon. The results of the fluorescence probe measurement and the secondary structure change by the addition of TFE can be well explained with this three-phase model, that is, the monomer−tetramer−micelle system. By means of temperature-scanning CD at various concentrations it has been proved that there exists an equilibrium of the tetramer and the micelle as well as that of the monomer and the micelle. Furthermore, this model can be confirmed by the dynamic light scattering data given by Dathe et al. (1996). Their figure shows the existence of the particle with the size of 15−30 nm besides the monomer and the tetramer, though this was not discussed by them. This micelle size corresponds to the association of about 1000−10 000 CRF molecules. Since they also reported that CRF forms antiparallel β-structure at 7 mM as well as α-helix, the micelle would be constructed with both intermolecular β-structure and helix−helix interaction.

In spite of the similarly amphipathic helices, the concentration dependency of CRF is quite different from the other peptides such as coiled-coils and helix-bundles (Ho et al., 1987; Kojima et al., 1996; Morii et al., 1997), which exhibit a clear concentration-dependent equilibrium between monomers and oligomers. The specific and intriguing feature of CRF tetramer may be attributed to its unique folding structure similar to the native proteins. In this study, it was revealed that the CRF tetramer is generated only through the micelles and not from the monomer directly.

In summary, it should be emphasized that the folding pathway of the tetramer demands the micelle state. This fact is very suggestive for the general protein folding problems. As for the thermodynamic folding pathway, several models are proposed so far: jigsaw puzzle model, diffusion−collision model, nucleation model, framework model, and hydrophobic collapse model (Karplus et al., 1992). The formation of CRF tetramer resembles the collapse model (Dill, 1985, 1990). The folding pathway of the CRF tetramer also includes some characteristics analogous to the in vivo folding by the aid of molecular chaperons, which bind molten-globular intermediates of proteins in their earlier folding stage (Buchner et al., 1991; Martin et al., 1991). As shown by ANS binding experiments, the CRF micelles bear the molten-globular characteristics. The micelle-driven folding of CRF seems to be essentially the same as the chaperon-driven folding in a sense, because both systems would utilize the molten-globule-based complexes first and then liberate the folded proteins from them.

This study contributes not only to revealing the CRF structure but also to clarifying the principle of protein folding and, moreover, the engineering of protein folding. In relation to the thermodynamical behavior of CRF as revealed in this study, the molecular mechanism of expressing physiological functions would become much more interesting and significant.

ACKNOWLEDGMENT

We are grateful to Dr. Kunihiro Kuwajima (University of Tokyo) for valuable discussions and to Mr. Tatsuyuki Takenawa for ESI-MS measurement. The secretarial assistance of Ms. Akemi Kamiya is gratefully acknowledged.

REFERENCES

Betz, S. F., & DeGrado, W. F. (1996) *Biochemistry 35*, 6955−6962.
Buchner, J., Schmidt, M., Fuchs, M., Jaenicke, R., Rudolph, R., Schmid, F. X., & Kiefhaber, T. (1991) *Biochemistry 30*, 1586−1591.
Chen, Y.-H., Yang, J. T., & Chau, K. H. (1974) *Biochemistry 13*, 3350−3359.
Chou, P. Y., & Fasman, G. D. (1978) *Annu. Rev. Biochem. 47*, 251−276.
Dathe, M., Fabian, H., Gast, K., Zirwer, D., Winter, R., Beyermann, M., Schümann, M., & Bienert, M. (1996) *Int. J. Peptide Protein Res. 47*, 383-393.
Dill, K. (1985) *Biochemistry 24* , 1501−1509.
Dill, K. (1990) *Biochemistry 29* , 7133−7155.
Gillies, G., & Lowry, P. (1979) *Nature 278*, 463−464.
Guillemin, R., & Rosenberg, B. (1955) *Endocrinology 57*, 599−607.
Handel, T. M., Williams, S. A., & DeGrado, W. F. (1993) *Science 261*, 879-885.
Herzfeld, S. H., Corrin, M. L., & Harkins, W. D. (1950) *J. Phys. Colloid Chem. 54*, 271−283.
Ho, S. P., & DeGrado, W. F. (1987) *J. Am. Chem. Soc. 109*, 6751−6758.
Karplus, M., & Shakhnovich, E. (1992) in *Protein Folding* (Creighton, T. E., Ed.) Chap. 4, W. H. Freeman and Company, New York.
Kidokoro, S., & Wada, A. (1987) *Biopolymers 26*, 213−229.
Kidokoro, S., Uedaira, H., & Wada, A. (1988) *Biopolymers 27*, 271−297.
Kojima, S., Kuriki, Y., Sato, Y., Arisaka, F., Kumagai, I., Takahashi, S., & Miura, K. (1996) *Biochim. Biophys. Acta 1294*, 129−137.
Lau, S. H., Rivier, J., Vale, W., Kaiser, E. T., & Kézdy, F. J. (1983) *Proc. Natl. Acad. Sci. U.S.A. 80*, 7070−7074.
Lau, S. Y. M., Taneja, A. K., & Hodges, R. S. (1984) *J. Biol. Chem. 259*, 13253−13261.
Martin, J., Langer, T., Boteva, R., Schramel, A., Horwich, A. L., & Hartl, F.-U. (1991) *Nature 352*, 36−42.
Morii, H., Takenawa, T., Arisaka, F., & Shimizu, T. (1997) *Biochemistry 36*, 1933−1942.
Ohashi, S., Shiraki, M., Okada, M., & Munekata, E. (1983) *Peptide Chem. 1982*, 143−148.
Pallai, P. V., Mabilia, M., Goodman, M., Vale, W., & Rivier, J. (1983) *Proc. Natl. Acad. Sci. U.S.A. 80*, 6770−6774.
Romier, C., Bernassau, J.-M., Cambillau, C., & Darbon, H. (1993) *Protein Eng. 6*, 149−156.
Sayers, G., Hanzmann, E., & Bodanszky, M. (1980) *FEBS Lett. 116*, 236−238.
Schally, A. V., Andersen, R. N., Lipscomb, H. S., Long, J. M., & Guillemin, R. (1960) *Nature 88*, 1192−1193.
Spiess, J., Rivier, J., Rivier, C., & Vale, W. (1981) *Proc. Natl. Acad. Sci. U.S.A. 78*, 6517−6521.
Vale, W., Spiess, J., Rivier, C., & Rivier, J. (1981) *Science 213*, 1394−1397.

BI9712293